ARTICLE

Proteomic Patterns and Transcriptional Evaluation Reveals Prognostic Potential of Novel Serum Biomarkers in Progression of Prostate Cancer

Farheen Waziri[1], Archana Kumari[2], Nimisha Gupta[3], Sarfaraz Ali[4], Sangeeta Pal5 Saima Wajid[6*], Raj Kumar[7*]

[1]*Assistant Professor, Department of Zoology, G.B.M. College Gaya, Magadh University Bodh-Gaya, Bihar, India*
[2]*Assistant Professor, Department of Zoology, Gaya College Gaya, Magadh University Bodh-Gaya, Bihar, India*
[3]*Assistant Professor, Department of Biotechnology, University of Kota, Rajasthan, India*
[4]*P. G. Department of Biotechnology, Magadh University, Bodh-Gaya, India*
[5]*Assistant Professor, Department of Zoology, Brahmanand College, The Mall Kanpur Nagar, Uttar Pradesh*
[6]**Associate Professor, Department of Biotechnology, School of Chemical and Life Sciences, Jamia Hamdard*
[7]**Assistant Professor, S.N.Sinha College, Tekari, Magadh University Bodh-Gaya, Bihar, India*
**Co-corresponding authors*
***Corresponding author: Raj Kumar[7*] Saima Wajid,** raj12140in@gmail.com
[*]Co-corresponding authors

ABSTRACT

Objective: Aging population, stressfully transforming lifestyle and perturbed urological physiology are contributing to the recent incidence of anxious rise in prostate cancer (PCa) across the globe, including India. Despite of advancing knowledge and decades of applied urological research, the existing insights are insufficient to curb the menace. This very situation intrigued us to investigate and identify the differential and clinically relevant prognostic serum based biomarkers in induced animal model of PCa with an intention to contribute an insight in early and accurate detection and additive avenues for effective clinical case management. Methods: We employed 2-DE and MALDI-TOF-MS techniques followed by tissue diagnosis for pathophysiological characterization and disease differentiation that were assessed by histopathology and to corroborate the sustainable evidences of proteomics observations and to ascertain the functional association and regulation of corresponding genes; transcriptional genomics were performed using qRT-PCR. Results and Conclusion: We distinctly observed SRCIN1, DCAF6, PTP4A2 and MRPL15; novel and under investigated serum markers in protein profiling and time dependent differentially expressed patterns of respective genes in Wistar rat PCa tissues. We found significantly upregulated expression of MRPL15 and quite early pronounced shift (4.9 fold), suggesting specificity and efficiently early tumour inducer candidate marker; whereas DCAF6, though showed overall upregulation, but pronounced and noticeable shift (7.8 fold) was observed quite late; suggesting time dependent sensitivity as marker's characterization of late tumour inducer candidate. Further, SRCIN1 were down regulated irrespective of time course, whereas PTP4A2 were also down regulated but quite late and marginally showed non-significant upregulation (<0.5 fold); suggesting specificity of SRCIN1 and PTP4A2, as tumour suppressor marker. However, PTP4A2 may have dichotomic potential as quite late phase tumour inducer marker candidate as well. In conclusion, these proteins may therefore possess a potential candidature in improving PCa diagnosis during its early stage. Further functional and clinical validation studies of these cancer-associated proteins are necessary to elucidate their precise role in the process of prostate carcinogenesis.

Keywords: Prostate cancer, PIN, Proteomic analysis, 2D, MALDI-TOF-MS, Wistar rat

How to cite this article: Waziri F, Kumari A, Gupta N, Ali S, Pal S, Wajid S, Kumar R., Proteomic Patterns and Transcriptional Evaluation Reveals Prognostic Potential of Novel Serum Biomarkers in Progression of Prostate Cancer. Int J Drug Deliv Technol. 2026;16(77s): 1808-1822; DOI: 10.25258/ijddt.16.77s.207

INTRODUCTION

Prostate cancer (PCa) is the most commonly diagnosed urological malignancy and is the second most common cancer in men. More than 1.1 million men worldwide were diagnosed with PCa in 2012, accounting for 15 percent of the cancers diagnosed in men, with almost 70 percent of the cases (759,000) occurring in more developed regions [1]. In United States it is the second leading cause of cancer deaths in men [2]. According to American Cancer1 Society, an estimated 164,690 new cases of PCa will be diagnosed and 29,430 men will die of PCa in 2018 [3]. In India also, PCa is the second most common cancer in males as per the Indian Council of Medical Research (ICMR) and different state cancer registries. As per Urological Oncology (March 24, 2017), the rates of incidence are constantly and rapidly increasing and the cancer projection data (projected cases estimated 26,120 and 28,079 for the year 2010 and 2015 respectively) shows that by 2020 the number of cases will become double. The serum PSA (prostate specific antigen) test and abnormal DRE (digital rectum examination) despite being widely used as a first-line for screening PCa in the last decade [4], lacks sensitivity and specificity [5], as it is unable to determine whether PCa is in indolent or aggressive form [5]. These diagnostics tests are suboptimal resulting in over diagnosis and overtreatment of many clinically insignificant prostate cancers [6]. In preview of limitations of PSA, several prostate cancer biomarkers have been identified till now, [7] but these are required to be validated clinically prior to the routine use [8, 9]. Therefore, additional biomarkers are needed to be explored in order to overcome these limitations and improve the early detection and prognosis.[10] To diagnose cancer in its early stage proteomics-based study are becoming increasingly popular.[11] In order to identify the differentially expressed proteins during transition from normal to neoplastic stage, proteomic analysis has provided new insights to study the changes that occur during early phase of

cancer progression, giving rise to candidate biomarkers for prognosis and improved response to treatment.[12]

The advancement in proteomic technologies has resulted in utilizing serum as a highly desirable source to discover clinically useful biomarkers.[10] In opposition of the stable nature of the genome, the proteome of serum is considered dynamic, since the expressed proteins, native, fragmented, or post translationally modified, change quickly in response to pathogenic stimuli [13]. Although prostate cancer tissue biopsy is considered gold standard of cancer diagnosis, there is high risk of low tolerance, invasive sampling and significant mortality risk [14]. Due to minimally invasive and very low cost procedure to collect serum samples, screening of serum can be highly desirable in order to identify prostate cancer biomarkers.

Despite of extensive ongoing investigation across the globe, there are limited published studies elucidating the actual mechanistic initiation and progression of prostate cancer. This very existing knowledge gap, necessity of prompt clinical diagnosis and therapeutic intervention; rationally raised the requirement of systematic investigation towards the development of reliable preclinical disease model. Among few documented studies on preclinical disease models [15-17]; the investigation carried out using animal model by Peixoto et al [18] was very much in accordance with our study design. We have used Wistar rats for induction and evaluating the events of progression of prostate cancer using chemical carcinogen, N-Methyl,N-Nitrosourea (MNU) in addition to testosterone and cyproterone acetate. Following standard protocol for chemically induced carcinogenesis in animal model; we have successfully observed the initiation of PCa lesions mainly in the dorsolateral lobe of rat prostate, very much homologous region to the human prostate cancer [19, 20]. The early stage prostate tumorigenesis in Wistar rat model closely mimics the human condition recapitulating many aspects of human PCa which include prostate lobes enlargement, hyperplasia of stroma with moderate inflammation, ductal dilations, dysplasia, prostatic intra-epithelial neoplasia (PIN), and finally development of adenocarcinoma

21-24

.

In the present study, we developed chemically induced prostate cancer Wistar rat model to investigate serum-based biomarkers, using proteomic approaches – 2D electrophoresis and mass spectrometry. 2D-PAGE being traditionally employed to explore potential biomarkers related with large number of cancers including ovarian [25], lung [26], pancreatic [27], colorectal [28] and oral squamous cell carcinoma [26], it is still a highly popular technique to analyze protein expression levels between healthy and diseased state [28]. We employed 2-DE and peptide mass fingerprinting based on MALDI-TOF-MS techniques adopting proteomics approach, tissue diagnosis for pathophysiological characterization and disease differentiation were assessed by histopathology and to corroborate the sustainable evidences of proteomics observations and to ascertain the functional association and regulation of corresponding genes; transcriptional genomics were performed using qRT-PCR with the aim of identifying novel, PCa associated proteins

(biomarkers) during early stages of disease.

RESULTS GENERAL OBSERVATION

All animals remained healthy throughout the experimental period, except for certain changes seen in induced rats in comparison to untreated control rats in terms of body weight. Histologically, there were no pathological alterations due to CA+TP+MNU treatment in other organs of the animals. Gross observation of rat prostate gland showed prostatic enlargement while histopathological evaluation showed spectrum of changes in CA+TP+MNU treated rats which had affected the dorsolateral lobe. Differential expression in serum proteome was observed during early pre-neoplastic stage and worked upon. **Body weight and prostatic weight analysis**

Figure 1 represents the Wistar rats' average body weight during CA+TP+MNU induced prostate carcinogenesis. A significant body weight gain suppression was observed in induced rats compared to untreated control animals (Figure 1). Body weight started declining from 13 months onwards and continued till end i.e. 19 months. The dorsolateral prostatic weights were significantly increased in treated rats during prostate carcinogenesis as depicted in Figure 2.

HISTOLOGICAL RESULTS

H&E stained sections: The histological findings showed that control rats, as expected did not develop adenocarcinoma. The microscopic examination as illustrated in figures (3A & B) showed uniformly sized glands set in a loose fibrous stroma. The tubules of the dorsolateral prostate (DLP) were lined by a single layer of cuboidal cells with secretions in the lumen. There were no inflammatory cell infiltrations in stroma or the epithelial lining of the glands. Multilayering and any atypical features were also not seen. The dorsolateral lobe of CA+TP+MNU treated rats developed benign epithelial hyperplasia, pre-neoplastic [low grade prostatic intraepithelial neoplasia (LGPIN or PIN1) and high grade prostatic intraepithelial neoplasia (HGPIN or PIN 2 and3)], and neoplastic (adenocarcinoma) prostate lesions from 13 months onwards. Such lesions were not found in other control prostatic lobes. The rats sacrificed post 13 months showed hyperplastic changes showing thickening of the epithelium and the formation of papillary processes (Fig.3C). High magnification (Fig.3D) showed mild variation in nuclear size, however, the nuclear arrangement was regular and no multilayering or any other atypical features was seen. The next sacrifice lot post 15 and 17 months (Fig.3E, F and 4 C, D) observed LGPIN and HGPIN. Low power photomicrograph (HE x 100) from prostate gland of these groups of animals showed a prostatic gland with features of epithelial hyperplasia. In these samples also, the epithelium projected into the lumen of the gland in folds. Some of the folds showed multilayering of the glandular epithelium. High power photomicrograph (HE x400) of the same section showed the hyperplastic glandular epithelium. These low grade PIN showed cells within ducts are heaped and irregularly spaced with marked variation in nuclear size. The nuclei of the epithelial cells were enlarged and showed variation in size and shape. However, the nuclei were devoid of nucleoli. These features were also observed in groups of animals sacrificed post 17 months, however nuclei were enlarged, hyperchromatic and showed variation in size and shape and most importantly showing prominent nucleoli (arrow) – a hallmark of high grade prostatic intraepithelial neoplasia (Fig. 4D). The full- fledged neoplastic lesions were observed after 19 months (Fig. 4E & F)) which showed more active glandular activity filling the entire lumen with folds of hyperplastic epithelium fusing together to form sheets of cells. However there in no stromal extension, but heavy inflammatory infiltrate is seen in stromal tissues when seen under low magnification (x100). High power from the same section shows a focus of adenocarcinoma in the gland. The epithelial cells here have large dark and irregular shaped nuclei. The arrow shows a mitotic figure. The cells have coalesced to form small sheets of atypical cells. Nucleoli are prominently seen. However, control post 19 months lacked any such changes except for some old ages changes, like irregularly infolded epithelial projections in the lumen (Fig. 4 A&B).

PROTEOMIC ANALYSIS

One-dimensional gel electrophoresis: Fig 5 illustrates the separation of serum samples collected in 13 months showed significant differential protein profile, however the earlier interval collections did not show any significant differences in protein profile. A differential band pattern was observed in CA+TP+MNU treated (T1 and T2) samples compared to control (C) sample. The bands shown in Lane T1 were found to be differential with thickness and intensity visibly higher in the 1D profile of treated in comparison to the control. Stain intensity and band thickness were lower in Lane T2 corresponding to control whereas there was

unique absence of band in Lane C as compared to treated. The samples expressing differential pattern (N=12) were selected, rerun twice for confirmation, and were processed so forth for 2D gel electrophoresis.

Two-dimensional gel electrophoresis: 2D gel electrophoresis were performed in triplicates on serum of control and CA+TP+MNU treated samples yielding reproducible results. Figure 6 shows a representative silver-stained 2D protein profiles of serum from control(Fig6A) and treated (Fig6B). Significant changes in the levels of some CA+TP+MNU treated serum proteins compared to control were seen.

An apparent difference in protein spot area and intensity was visible on 2D SDS-PAGE gels as shown in Figure 6. Both gels profiles were analyzed by PDQuest software which generated master gel image containing all the spots found in control as well as treated samples. The four differential spots selected for further analysis were SSP1105, SSP5104, SSP2006 and SSP7006 (Table S2 SI Dataset). The spot (qualitative) SSP1105 was present in both gels and had significantly higher intensities compared to control. The spots (qualitative) SSP5104 and SSP2006 were present in both gels and had significantly lower intensities compared to control. The spot SSP7006 (qualitative) was present only in the 2D gel of treated sample. The protein intensities of the selected spots as calculated by the PD quest software(Bio-Rad), were statistically meaningful ($p < 0.05$). The evaluated protein intensities of selected spots were: 'SSP1105': 118275 intensity (INT) x area; 'SSP5104': 42016 intensity (INT) x area; 'SSP2006': 131990 intensity (INT) x area; and 'SSP7006': 34746 intensity (INT) x area. The 3D view of the expressed spots (Figure 7) further validates the SSP calculations. **Protein identification by MALDI-TOF MS**

The target spots excised from 2D gels were peptide mass fingerprinted and characterized by MALDI-TOF MS, which led to the identification of SSP 1105 as 39S ribosomal protein L15, mitochondrial isoform X1 or MRPL15; SSP 5104 as Protein tyrosine phosphatase type IVA 2 or PTP4A2; SSP 2006 as SRC kinase signaling inhibitor 1 or SRCIN1 and SSP 7006 as DDB1- and CUL4-associated factor 6 isoform X2 or DCAF6 in *Rattus norvegicus*. The experimental molecular weight of these proteins were found to be slight different from the theoretical molecular weight (Table S2 SI Dataset). Such a discrepancy may attribute to post translational modifications, most likely glycosylation, which has an impact on electrophoretic mobility or it may also be due to cleavage of signal peptides and propeptides [29]. The table S3 (SI Dataset) contains list of all peptide sequences, including any deviations from expected cleavage specificity.

QRT (QUANTITATIVE REAL TIME)-PCR VALIDATION

Based on the findings of 2-dimensional electrophoretic characterization of serum protein markers, we observed that transcriptional precursors of these genes i.e. MRPL15, SRCIN1, PTP4A2 and DCAF6 serum proteins are potentially prominent in chemically induced progression of prostatic malignancy as compared to non-induced control tissue. These proteins are actively engaged in cellular death processes, autophagy, downstream signaling cascade, orchestrating cellular energy and metabolism, regulation of tumour suppressor genes, and mediating various other cellular machineries in normal and augmented cells. In view of the identified cellular components and in order to understand the functional expression and impact of these proteins on its regulation in augmented cellular process i.e. during the progression of malignancy; we analyzed the transcriptional expression of *MRPL15*, *SRCIN1*, *PTP4A2* and *DCAF6* genes, using RNA from dorsolateral lobe tissue of adult male Wistar rats in time dependent stratified group of animals as compared to control group of animals by employing qRT-PCR.

We observed overall upregulated expression of MRPL15 mRNA in induced tissue, as shown in Figure-8. We found differential expression of MRPL15 transcript across the time dependent induction and the differences were statistically significant as compared to non-induced tissue group, as shown in Figure-8A. However, 13month post induction sacrificed animal's tissue has shown 2.6 fold increased expression, followed by 4.1 and 4.3-fold expression in 17 and 19month post induction sacrificed animal's tissue, respectively; whereas peak of highest fold change i.e. 4.9 was observed in case of 15-month post induction sacrificed animal's tissue relative to non-induced control tissue, as shown in Figure-8B. Thereafter, we observed down regulated expression of PTP4A2 mRNA in induced tissue, as shown in Figure-9. We found differential expression of PTP4A2 transcript across the time dependent down regulation and the differences were statistically significant only in case of 13 and 17 months' post induction sacrificed animal's tissue as compared to non-induced tissue group, as shown in Figure-9A. However, 15-month post induction sacrificed animal's tissue has shown 0.1 fold decreased expression, followed by 0.3 and 0.3-fold expression in 13 and 17 months' post induction sacrificed animal's tissue, respectively; whereas marginal upregulated fold change was also observed i.e. 0.1 was observed in case of 19-month post induction sacrificed animal's tissue relative to non-induced control tissue and the differences were non- significant, as shown in Figure-9B and 9A. Further, we observed overall down regulated expression of SRCIN1 mRNA in induced tissue, as shown in Figure-10. We found differential expression of SRCIN1 transcript across the time dependent down regulation and the differences were statistically significant as compared to non-induced tissue group, as shown in Figure-10A. However, 15-month post induction sacrificed animal's tissue has shown 0.4 fold decreased expression, followed by 0.2 and 0.6-fold expression in 17 and 19-month post induction sacrificed animal's tissue, respectively; whereas peak of highest fold change decrease i.e. 0.7 was observed in case of 13month post induction sacrificed animal's tissue relative to non-induced control tissue, as shown in Figure-10B.

Furthermore, we observed overall upregulated expression of DCAF6 mRNA in induced tissue, as shown in Figure-11. We found differential expression of DCAF6 transcript across the time dependent induction and the differences were statistically significant as compared to noninduced tissue group, as shown in Figure-11A. However, 13-month post induction sacrificed animal's tissue has shown 1.6 fold increased expression, followed by 1.6 and 1.4-fold expression in 15 and 17-month post induction sacrificed animal's tissue, respectively; whereas peak of highest fold change i.e. 7.1 was observed in case of 19-month post induction sacrificed animal's tissue relative to non-induced control tissue, as shown in Figure-11B.

DISCUSSION

Prostate cancer – a major cause of cancer related death in men globally, targets to explore potential non-invasive serum biomarkers for accurate diagnosis of PCa [30]. The identification of novel biomarkers for various cancer including prostate cancers have been well explored using proteomics approach [31], and the comparative serum proteome based prostate cancer biomarkers search have been applied by several groups, [32]. In this study, we attempted to explore the altered expression of serum proteins of control subject in compared to induced during early stages of the disease through pre-clinical studies.

We get more reliable information from clinical samples analysis, but the heterogeneous and multifactorial nature of clinical samples demands a large number of samples to obtain statistically significant data. Moreover, due to difficulty in accessing tumour specimens displaying early stages of tumorigenesis, study of differentially expressed proteins during early stages in preclinical models was an alternative choice in our proteomics approach.[33, 34] CA+TP+MNU induced rat prostate cancer was developed using a well – established animal model.[35] CA+TP+MNU induces a multi-step processes of carcinogenesis which clearly showed hyperplasia, dysplasia, PIN (prostate intraepithelial neoplasia) and ultimately adenocarcinoma – counter part of the disease in man, in the dorsolateral lobe of prostate gland. [36]. In our study we successfully constructed this PCa model. For proteome analysis,

serum samples from CA+TP+MNU-treated animals and healthy control were collected at different time intervals and were processed further which enabled us to study the differentially expressed proteins during early stages of prostate carcinogenesis. As per the data/literature reviewed, there are hardly any reports available regarding the serum proteome analysis during early stages of PCa in *in vivo* model. In search of exploring some novel, candidate proteins (markers) for PCa early diagnosis, we analyzed the serum proteome using SDS-PAGE coupled with MALDI-TOF-MS analysis. Screening of serum proteome by one dimensional gel electrophoresis showed that the samples collected during 13 months of model development displayed significant changes in protein expression profiles. The selected samples were further resolved by two-dimensional gel electrophoresis, and the differentially expressed proteins were spotted by PDQuest software analysis. We identified four differentially abundant, statistically significant gel spots (SSP 1105,

SSP 5104, SSP 2006 and SSP 7006). Among these, SSP 1105 and SSP 7006 showed upregulation, while SSP 2006 and SSP 5104 were downregulated in treated samples as compared to control healthy subject. These spots were further selected for MALDI-TOF MS- based PMF analysis. The identified proteins are tabulated in Table S2 (SI). The expression changes were further validated using qRT-PCR, which was found to be consistent post 15, 17, and 19 months of model development.

In view of the identified cellular components and in order to understand the functional expression and impact of these proteins on its regulation in augmented cellular process i.e. during the progression of malignancy; we analyzed the transcriptional expression of *MRPL15, SRCIN1, PTP4A2* and *DCAF6* genes, using RNA from CA+TP+MNU induced prostatic

dorsolateral lobe tissue in time dependent stratified group of animals as compared to noninduced control group of animals by employing qRT-PCR. The isoform X1 of Mitochondrial Ribosomal Protein L15 or 39S mitochondrial ribosomal protein L15(MRPL15) is one of more than seventy protein components of mitoribosome complex that are encoded by the nuclear genome (nuclear gene Mrpl15). Mitochondria are important for apoptosis and autophage which are key processes in cancer cell. Energy production through the oxidative phosphorylation (OXPHOS) system, and regulation of the intrinsic pathway of apoptosis are the fundamental attributes of mitochondria [37]. Dysregulations in these functional attributes are described as the hallmark of cancer, and any changes in these processes leads to growth of cancer cells largely by producing energy through glycolysis and escaping intrinsic apoptotic pathways [38]. The aberrant expression of mitoribosomal proteins has been reported in various types of cancer including PCa

39

. It has already been reported that mitoribosomal proteins L15 level increases in liver cancer, lung cancer and melanoma [39],while that of MRPL36 shows decreased level in breast, colon and pancreatic tumour [39].The expression level of MRPL20 has been observed significantly downregulated in androgen-independent prostate cancers [40]. Inspite of differential mitoribosomal proteins abundance seen among different forms of cancer, some individual mitoribosomal proteins have potential candidature to be considered as diagnostic markers based on genomewide association studies (GWAS) and proteomics studies. [39]. uL11m (MRPL11) is considered a potential cancer biomarker in progression of head and neck squamous cell carcinoma (HSNCC), as it is associated with decreased MRPL11 expression [38]. In colorectal tumorigenesis the expression of several MRP genes have been reported as potential prognostic marker [41]. As several mitoribosomal proteins have pro-apoptotic roles, and many others are differentially expressed during tumorigenesis, MRPL proteins have the potential of becoming tumour-specific biomarkers. The finding of our study reports altered expression of MRPL15 right from early stage which might suggests its potential utility to be considered as prognostic marker for early detection of cancer. We found significantly upregulated expression of MRPL15 and quite early pronounced shift (4.9 fold), suggesting specificity and efficiently early tumour inducer candidate marker. As far as our knowledge the overexpression of MRPL15 and its role in in prostate tumorigenesis has not been reported elsewhere [39], ascertaining it as a novel protein showing altered level in prostate cancer.

The protein tyrosine phosphatase type IVA, member 2, encoded by nuclear gene PTP4A2 (1p35.2), belongs to a small class of the protein tyrosine phosphatase 4A (PTP4A) family [or phosphatase of regenerating liver (PRL phosphatases)]. PTPs exerts variable effects on signaling pathways [42], thus playing role in regulation of varieties of cellular processes. These molecules possess a catalytic domain (tyrosine phosphatase) and a characteristic C-terminal prenylation motif. They help in regulation by interacting with the subunit of Rab geranylgeranyl transferase II (beta GGT II). In nasopharyngeal carcinoma tumour progression is correlated with overexpression of phosphatase of regenerating liver-3 (PRL-3) [43], while in gastric cancer it is responsible for metastasis [44]. Moreover, a recent *in vitro* studies shows up-regulation of PRL-3 mRNA in prostate cancer tissue in comparison to normal prostate tissue, implying its role in PCa pathogenesis [45]. Although PTP4A1 and PTP4A3 have shown to be very important in development of cancer, the role of its close family member PTP4A2 is still largely unknown. Very few studies report the role of PTP4A2 in human cancer types. Recently, up-regulation of PTP4A2 (PRL-2) has been found in several types of cancers, especially of colon [46], pancreatic [47] and breast malignancy [48]. A very recent study shows the overexpression of PTP4A2 and its role in prognostication of NPC (nasopharyngeal carcinoma) [49]. We established 0.3 fold downregulated expression of transcriptional PTP4A2 mRNA in early stage (13 months' post carcinogen administration) prognosis of prostate cancer (p value = 0.001). However, with the advancement of tumor progression showing characteristic higher motility, invasion, and metastasis of the cancerous cells; PTP4A2 levels were further reported to be upregulated hence also favoring its dichotomic role as a biomarker in late phase of prostate tumour.

Originally defined as SNIP, SRC kinase signaling inhibitor 1 (SRCIN1), also named as p140CAP (p140Cas- associated protein) is a multi-site docking protein possessing N-terminal tyrosine-rich region, a putative actin -binding domain, a proline- rich domain (Pro 1), a coilcoiled region, two highly charged amino acid regions, and a C-terminal proline-rich domain (Pro 2) [50, 51]. Encoded by *SRCIN1* gene (17q12) it causes inactivation of Src and functions as a tumor suppressor gene in various cancers [52]. It inhibits Src activity and downstream signaling by activating CSK which leads to impaired cell spreading and migration [53]. A study by Chen et al [54] demonstrated that proliferation and epithelial-mesenchymal transition in human liver cancer occurs due to downregulation of SRCIN1 expression which is exhibited by miRNA-32 while by miR-150 in lung cancer [55]. Its role in tumour suppressor has also been in seen in highly metastatic breast cancer cells which is accomplished by inhibiting cortactin-dependent cell motility [51]. A recent study shows downregulation of SRCIN1 in osteosarcoma cell lines and tissues signifying its role as a novel tumor suppressor gene [56]. These studies very clearly demonstrate the role of SRCIN1 is regulating cell proliferation and motility, however there isn't any report regarding its role in prostate cancer. Here, we reported differential expression of SRCIN1 transcript with sharp decline in downregulated signaling (p-value = 0.001) in early stage (13 months' post carcinogen administration) of cancer while, such patterns were also maintained throughout different stages of cancer advancement in prostate tissues (p-value = 0.002). Our data suggests the specificity of SRCIN1 as a tumor suppressor marker in prostate cancers, however, further studies are required to explore its role with its interacting proteins and their effects in regulation of cell proliferation in prostate tumorigenesis.

The isoform X2 of DDB1- and CUL4-associated factor 6 (DCAF6) protein, encoded by the nuclear gene *DCAF6*, was found to be overexpressed in early stages of prostatic neoplasm than in non-neoplastic control. DDB1 or damage-specific DNA binding

protein 1 is a multifunctional protein that helps in maintaining cell cycle progression and genome integrity. It is a part of damaged DNA binding protein complex (other part is DDB2). DDB1, a triple β-propeller adapter protein is used as a linker by CUL4 (the cullin family protein) to recruit substrates or substrate receptors to form CUL4-RING3 (or CUL4E3) ubiquitin ligase complex, This complex assists in regulating selective proteolysis of key proteins that are responsible for DNA repair, replication and transcription [57]. Found in CUL4-RING E3 ubiquitin ligase complex DCAF6 protein is associated with cerebral visual impairment, intellectual disability and prostatic neoplasms. (rgd.mcw.edu/rgdweb/report/gene/main.html? id =1561961). It also functions as a liganddependent coactivator of glucocorticoid receptor (GR), nuclear receptor subfamily 3 group C member 1 (NR3C1) and androgen receptor (AR). The oncogenic role of CUL4A (paralog of CUL4) is well established. Overexpression of CUL4A has been reported in many types of malignancies such as squamous cell carcinoma, adrenocortical carcinoma, breast cancer, hepatocellular carcinoma, childhood medulloblastoma as well as prostate cancer [58]. Recently, a number of DCAFs (DDB1-CUL4 associated factors) of DDB1-CUL4 associated factors family have been identified [59], and have been found to have role in different types of malignancies: DCAF1 is associated with hepatitis c virus (HCV) infection, DCAF13 having prognostic role in hepatocellular carcinoma, and elevated expression of DCAF16 have been seen in urothelial carcinoma, adenocarcinoma, and squamous cell carcinoma [60, 61]. However, the specific involvement of DDB1-CUL4A associated factors role in cancer progression requires further studies. A recent study has shown that mRNA expression level (gene copy number) of DCAF6, 7, 8, 13, and 17 are upregulated whereas that of DCAF10, 12 and 15 are decreased or lost frequently in lung adenocarcinomas [62]. In breast cancer tissue, high expression level of DCAF6 (also named NRIP) are significantly associated with adverse clinical outcome [63], while study by Han et al showed its high expression in skin, ovarian, colon, esophageal and pancreatic cancer [64]. The role of DCAF6 in association with androgen receptor proteins (AR) has recently been studied in certain specific types of aggressive prostate cancer, where high expression levels of DCAF6 along with AR proteins, displaces DDB2 (DNA damage binding protein2) from CUL4A-DDB1 E3 ligase complex contributing to the pathogenesis of prostate cancer [65]. There are dearth of evidences regarding up-regulation of DCAF6 at precancerous stages of prostate cancer. The over-expression of DCAF6 right from early stage of prostate carcinogenesis, favors its role in early detection (prognostication) of prostate cancer. DCAF6, though showed overall up-regulation, but pronounced and noticeable shift (7.8 fold) was observed quite late; suggesting time dependent sensitivity as marker's characterization of late tumour inducer candidate. **Conclusion**

In conclusion, by developing a well-established rat prostate cancer model, we analyzed the differential protein expression pattern of induced group in comparison to control group and identified novel set of proteins at very early stages of carcinogenesis by proteome analysis using 2-DE and MS techniques. These proteins may therefore possess promising relevance in improving PCa diagnosis during its early stage. The in-depth role of these proteins associated with cancer progression are necessary in order to mark them potential candidature as biomarkers. Ultimately, such proteins (biomarkers) may assists clinicians in diagnosing prostate cancer during its promotion stages and preventing unnecessary biopsy and overtreatment.

METHODS CHEMICALS

Chemicals Androcur tablets (50 mg Cyproterone acetate per tablet) were purchased from BAYER (Bayer Schering Pharma) and Testosterone propionate (used as a solution dissolved in Ricinus oil) was obtained from HIMEDIA. MNU (N-Methyl-N-Nitrosourea) was purchased from Sigma-Aldrich Co., USA. All other chemicals used were of analytical grade. **Ethics statement**

Before starting the study, the experimental protocol was reviewed and approved by the Institutional Animal Ethics Committee (IAEC) constituted as per directions of the Committee for the Purpose of Control and Supervision of Experiments on Animals (vide memo no.173/GO/Re/S/2000/CPCSEA, dated 03-03-2014), and ethical guidelines as reflected in the guidelines of CPCSEA. The animals were provided by "Central Animal House Facility" (CAHF), Jamia Hamdard, and the Approval ID/project number for this study is 1025. All aspects like animal care, use and welfare were followed.

ANIMALS

Male random-bred specific-pathogen-free adult Wistar rats weighing 100-150gm (8 weeks old), obtained from CAHF of Jamia Hamdard, New Delhi were housed under standard conditions, in stainless steel wire mesh cages (four per cage) having constant 12 h light and 12 h dark schedule at an ambient temperature of 20 ±2 °C and 50 ±10 % relative humidity. At all times during the studies the rats had ad libitum access to standard laboratory chow and water. **Experimental design**

A total of 36 rats were divided into 2 groups: Control healthy group (CHG) and Induction group (IG). In CHG the number of animals were 10, while in IG there were 26. Animals were distributed into experimental groups using a randomization process designed to ensure comparable mean initial body weights in all groups.

PROSTATE CANCER INDUCTION USING CARCINOGEN AND HORMONE

The protocol for induction of prostate cancer was modified from Bosland et al [35]. First, each rat of IG received daily, suspension of cyproterone acetate (CA) containing Androcur tablets dispersed in tap water for 18 consecutive days by gavaging, at a dose of 50mg/kg. The suspension was constantly stirred and the gavaging syringe was swirled until just before gavaging. After the final dose of CA treatment, they received daily subcutaneous injections of 100 mg Testosterone propionate(TP) in Ricinus oil per kg body weight for three days i.e. on days 19, 20, and 21 of the experiment. On day 22 the animals received a single intra venous dose (30mg/kg body weight) of MNU (prepared fresh) in the tail vein. Control healthy group animals were administered Ricinus oil subcutaneously during TP dose of IG, while normal saline intravenously during MNU treatment of IG. All the animals were checked daily and their body weight were recorded from 13 months onward. The experiment was terminated after 19 months. After each 13, 15, 17, and 19 months' animals were sacrificed by cervical dislocation under ether anesthesia effect. The prostate gland was removed, and dorsolateral lobes were separated, washed with saline, weighed accurately, and were fixed in 10% neutral buffered formalin (for histopathological examination) and RNA later (for RNA isolation). At the end of 19 months' all vital organs in addition to prostate were excised from all the sacrificed animals for the same purpose.

HISTOLOGICAL STUDIES

The dorsolateral lobe of prostate and other organs excised were fixed in 10% neutral buffered formalin. For sectioning and staining with hematoxylin and eosin (H&E) the specimens were subjected to at least 24 h in fixing solution and were then dehydrated in ascending grades of ethanol, cleared in benzene, and embedded in paraffin wax. Using xylene and ethanol the prostate tissue sections were deparaffinized and after washing the slides with phosphate buffered saline (PBS), these were permeabilized with permeabilization solution (0.1 M citrate, 0.1% Triton X-100). The sections were examined under light microscope at 100X and 400X magnifications to investigate the histopathological changes in prostate dorsolateral lobe tissue. **Proteomic analysis**

PREPARATION OF SERUM SAMPLES

After one month of completion of treatment schedule blood was collected from all animals every 30 days starting six months onwards. Animals were anesthetized with diethyl-ether and blood was drawn from their tail vein. Serum was collected from blood by centrifugation at 8000*g for 20 minutes and was further depleted

of abundant proteins using a dye based proteo-prep albumin and IgG depletion kit. The protein concentration in depleted serum samples was determined using Bradford micro assays [66].

ONE-DIMENSIONAL & TWO-DIMENSIONAL GEL ELECTROPHORESIS

The depleted serum samples were resolved by 12% SDS-PAGE system [67]. The samples containing 20 µg proteins were mixed with 2X protein loading buffer followed by heating at 90°C for 2 minutes and were further electrophoresed (in replicates) at a constant voltage of 150 V in the running buffer, Tris–glycine-SDS (pH 8.3). The resolved 1D profiles were visualized by standard protocols of silver staining.

For two dimensional gel electrophoresis the depleted serum samples were first resolved by isoelectric focusing using 11cm immobilized pH gradient (IPG) dry strips (GE Lifesciences) having pH range 4-7. The rehydration buffer containing 8 M urea, 2% CHAPS, 0.25% (v/v; pH 3-10) ampholytes (IPG buffer), 30 Mm dithiothreitol (DTT) and 0.1% bromophenol blue (BPB) was mixed with 100 µg of proteins sample making a final volume of 200µl per IPG strip. The strips were allowed to rehydrate with diluted samples overnight for 12-16 hour at RT. The proteins were then electrofocused by Ettan IPG phor II isoelectric focusing system (GE Healthcare) using a programmed voltage gradient at 20 with a current limit of 50 µA per strip under the given conditions: 500 V for 1 hour;1000 V for 1 hour;6000 V for 2 hours (gradient), and 6000 V for a total of 35,000 Vhrs. After IEF, the IPG strips were equilibrated in buffer 1 [30 % glycerol, 6 M urea, 2 % SDS, 75 mM Tris–HCl (pH 8.8), 0.002 % BPB,1% DTT] and buffer 2 containing 25% iodoacetamide instead of DTT in each case for 15 minutes. This was followed by SDS-PAGE. The equilibrated strips were transferred onto the top of 12% uniform SDS polyacrylamide gels (14 x16 cm) and sealed with 1% agarose prepared in SDS-Tris glycine buffer with traces of bromophenol blue as a tracking dye to monitor electrophoresis. Electrophoresis was performed with constant voltage (180V) in a running buffer (1X Tris– glycine-SDS, pH 8.3) until the dye front reached the bottom of the gel. The 2D gels protein spot profiles were visualized using standard protocol of silver staining [68], and were further scanned using Bio-Rad Versa Doc MP 4000 scanner followed by analysis using PD Quest 8.0 software

(Bio-Rad). Further the spots of interest were characterized using MALDI-TOF MS analysis.

MS ANALYSIS OF GEL SPOTS AND DATABASE SEARCH

In-gel digestion of proteins

Protein spots of interest were excised manually from the gel and were then destained by adding 15mM potassium ferricyanide and 50 mM sodium thiosulphate for 10 min interval (3-4 times). The gel pieces were dehydrated in acetonitrile, rehydrated in DTT solution in ammonium carbonate and reduced at RT for 0.5 h. DTT solution was removed and gel pieces were alkylated with IAA in ammonium bicarbonate at RT for 0.5 h followed by dehydration in acetonitrile for 10 min. After acetonitrile removal gel pieces were again rehydrated in ammonium bicarbonate for 10 min, and were again dehydrated in acetonitrile. Gel pieces were then completely dried by vacuum centrifugation for 10-15 min. A trypsin solution in ammonium bicarbonate was added in gel pieces for 30 min at RT followed by overlaying with ammonium bicarbonate and further incubation at 37° C for 16 h. Further recovery of the peptides was accomplished by two extractions with 50% acetonitrile along with 5% trifluoroacetic acid (TFA). The extract was evaporated using SpeedVac at 37° C for MS analysis.

MALDI-TOF MS and database search

Equal volume of the saturated solution of the HCCA (α-cyano-4-hydroxycinnamic acid) matrix in acetonitrile containing 0.1% TFA solution was mixed with tryptic digest in 1:1 and spotted onto the MALDI plate. After the sample was analyzed on MALDI-TOF/ TOF Ultraflex III, further analysis was done with peak list-generating software Flex Analysis software version 3.3 (build 80) for obtaining the peptide mass fingerprinting. The mass obtained in the peptide mass fingerprint was submitted to the MASCOT search engine for peptide mass fingerprint identification. Peptides were searched with reference to NCBInr (National Centre for Biotechnology non-redundant) database, taxonomy of *Rattus* for protein characterization. The protein score was _10 _ Log(P), where P is the probability that the observed match is a random event. Protein scores greater than 55 were selected to be significant ($p < 0.05$). **Quantitative real-time PCR analysis**

Total RNA was extracted from tissue using Mini SureSpin total RNA isolation kit (Nucleopore, Genetix Biotech Asia), with on-column DNase treatment. The cDNA (complementary DNA) was synthesized by reverse transcribing 1 µg of normalized RNA using manufacturers [(RevertAidTM First Strand cDNA Synthesis Kit (Thermo Fisher Scientific)] protocol. The cDNA integrity was checked by PCR using β-actin-specific primers (Table S1 SI) resulting in 207-bp amplicons. qRT-PCR was performed in the LightCycler 480 Real Time PCR System (Roche Applied Science) SYBR Green Master Mix (Thermo Fisher Scientific). Real-time PCR reaction was performed in triplicates for each sample and amplifications were carried out in a final volume of 25 µL including 12.5 µl of Maxima SYBR Green qPCR Master Mix, 0.4 µM of each primer (Table S1 SI), 1 µl of diluted (fivefold dilution) cDNA, and 9.5 µl of nuclease-free water. The thermal cycling conditions were (i) 95 °C for 5 min (initial denaturation), (ii) 40 cycles at 95 °C for 60 s, 55°C for 60 s, and 72 °C for 60 s, followed by (iii) melt curve analysis at a temperature range of 55°C - 95 °C. The raw data were analyzed using the LightCycler® 480 Software (Version 1.5). The data were analyzed using the $\Delta Ct(2-\Delta\Delta CT)$ method with control group as the calibrator and HPRT1 as the normalizer [56]. **Data analysis**

The data from individual groups were presented as means and standard deviations. Followed by, analysis of variance (ANOVA) test, for comparison of means of different groups by setting $p < 0.05$ as minimum criterion for statistical significance.

ACKNOWLEDGEMENT

: We sincerely acknowledge the financial support from the University Grant Commission (UGC-MANF) to Department of Biotechnology, Jamia Hamdard during the course of study.

Compliance with ethical standards

CONFLICT OF INTEREST

The authors declare that there is no conflict of interest.

REFERENCES

- Ferlay, J. et al. Cancer incidence and mortality worldwide: sources, methods and major patterns in GLOBOCAN 2012. *Int J Cancer* **136**, E359-386 (2015).
- Siegel, R.L., Miller, K.D. & Jemal, A. Cancer statistics, 2018. *CA Cancer J Clin* **68**, 7-30 (2018).
- Society, A.C. American Cancer Society. *Cancer Facts & Figures 2018; 2018* (2018).
- Banez, L.L. et al. Diagnostic potential of serum proteomic patterns in prostate cancer. *J Urol* **170**, 442-446 (2003).
- Mingkun Han, Z.L., Fang Wang, Ye Tao, Yehai Liu, Bao-Ling Adeam, Minbo Liu, Liyong Zhang. Idenfication of differencially expressed proteins from prostate cancer cell line by fluorescence 2D difference gel electrophoresis (2-D DIGE). *MOJ Cell Science & Report* **3**, 1-10 (2016).
- Norgaard, M. et al. Comprehensive Evaluation of TFF3 Promoter Hypomethylation and Molecular Biomarker Potential for Prostate Cancer Diagnosis and Prognosis. *Int J Mol Sci* **18** (2017).
- Iglesias-Gato, D. et al. The Proteome of Primary Prostate Cancer. *Eur Urol* **69**, 942-952 (2015).
- Davalieva, K. et al. Proteomics analysis of malignant and benign prostate tissue by 2D DIGE/MS reveals new insights

into proteins involved in prostate cancer. *Prostate* **75**, 1586-1600 (2015).
• Kim, Y. & Kislinger, T. Novel approaches for the identification of biomarkers of aggressive prostate cancer. *Genome Med* **5**, 56 (2013).
• Ornstein, D.K. & Tyson, D.R. Proteomics for the identification of new prostate cancer biomarkers. *Urol Oncol* **24**, 231-236 (2006).
• Simpson, R.J., Bernhard, O.K., Greening, D.W. & Moritz, R.L. Proteomics-driven cancer biomarker discovery: looking to the future. *Curr Opin Chem Biol* **12**, 72-77 (2008).
• Pin, E., Fredolini, C. & Petricoin, E.F., 3rd The role of proteomics in prostate cancer research: biomarker discovery and validation. *Clin Biochem* **46**, 524-538 (2013).
• Tessitore, A. et al. Serum biomarkers identification by mass spectrometry in high-mortality tumors. *Int J Proteomics* **2013**, 125858 (2013).
• Loeb, S. Prostate biopsy: a risk-benefit analysis. *J Urol* **183**, 852-853 (2010).
• Goncalves, B.F. et al. A new proposed rodent model of chemically induced prostate carcinogenesis: distinct time-course prostate cancer progression in the dorsolateral and ventral lobes. *Prostate* **73**, 1202-1213 (2013).
• Goncalves, B.F. et al. Prostate carcinogenesis induced by N-methyl-N-nitrosourea (mnu) in gerbils: histopathological diagnosis and potential invasiveness mediated by extracellular matrix components. *Exp Mol Pathol* **88**, 96-106 (2010).
• Sharmila, G. et al. Chemopreventive effect of quercetin in MNU and testosterone induced prostate cancer of Sprague-Dawley rats. *Nutr Cancer* **66**, 38-46 (2014).
• Peixoto, A.R. et al. Gestational and lactational exposition to Di-N-butyl-phthalate (DBP) increases inflammation and preneoplastic lesions in prostate of wistar rats after carcinogenic N-methyl-Nnitrosourea (MNU) plus testosterone protocol. *Environ Toxicol* **31**, 1185-1195 (2015).
• Shappell, S.B. et al. Prostate pathology of genetically engineered mice: definitions and classification. The consensus report from the Bar Harbor meeting of the Mouse Models of Human Cancer Consortium Prostate Pathology Committee. *Cancer Res* **64**, 2270-2305 (2004).
• McNeal, J.E. Normal histology of the prostate. *Am J Surg Pathol* **12**, 619-633 (1988).
• McCormick, D.L. & Rao, K.V. Chemoprevention of hormone-dependent prostate cancer in the Wistar-Unilever rat. *Eur Urol* **35**, 464-467 (1999).
• Bostwick, D.G., Pacelli, A. & Lopez-Beltran, A. Molecular biology of prostatic intraepithelial neoplasia. *Prostate* **29**, 117-134 (1996).
• Haggman, M.J., Wojno, K.J., Pearsall, C.P. & Macoska, J.A. Allelic loss of 8p sequences in prostatic intraepithelial neoplasia and carcinoma. *Urology* **50**, 643-647 (1997).
• Bosland, M.C., Prinsen, M.K., Dirksen, T.J. & Spit, B.J. Characterization of adenocarcinomas of the dorsolateral prostate induced in Wistar rats by N-methyl-N-nitrosourea, 7,12dimethylbenz(a)anthracene, and 3,2'-dimethyl-4-aminobiphenyl, following sequential treatment with cyproterone acetate and testosterone propionate. *Cancer Res* **50**, 700-709 (1990).
• Jones, M.B. et al. Proteomic analysis and identification of new biomarkers and therapeutic targets for invasive ovarian cancer. *Proteomics* **2**, 76-84 (2002).
• Tung, C.L. et al. Proteomics-based identification of plasma biomarkers in oral squamous cell carcinoma. *J Pharm Biomed Anal* **75**, 7-17 (2013).
• Rong, Y. et al. Proteomics analysis of serum protein profiling in pancreatic cancer patients by DIGE: up-regulation of mannose-binding lectin 2 and myosin light chain kinase 2. *BMC Gastroenterol* **10**, 68 (2010).
• Ghazanfar, S. et al. Identification of actin beta-like 2 (ACTBL2) as novel, upregulated protein in colorectal cancer. *J Proteomics* **152**, 33-40 (2017).
• Person, M.D. et al. Protein fragment domains identified using 2D gel electrophoresis/MALDITOF. *J Biomol Tech* **17**, 145-156 (2006).
• Zhang, M. et al. Combined serum and EPS-urine proteomic analysis using iTRAQ technology for discovery of potential prostate cancer biomarkers. *Discov Med* **22**, 281-295 (2016).
• White, N.M. et al. Quantitative proteomic analysis reveals potential diagnostic markers and pathways involved in pathogenesis of renal cell carcinoma. *Oncotarget* **5**, 506-518 (2014).
• Al-Ruwaili, J.A. et al. Discovery of serum protein biomarkers for prostate cancer progression by proteomic analysis. *Cancer Genomics Proteomics* **7**, 93-103 (2010).
• Ushijima, T. et al. Chromosomal mapping of genes controlling development, histological grade, depth of invasion, and size of rat stomach carcinomas. *Cancer Res* **60**, 1092-1096 (2000).
• Ohgaki, H., Kleihues, P. & Sugimura, T. Experimental gastric cancer. *Ital J Gastroenterol* **23**, 371377 (1991).
• Bosland, M.C. & Prinsen, M.K. Induction of dorsolateral prostate adenocarcinomas and other accessory sex gland lesions in male Wistar rats by a single administration of N-methyl-Nnitrosourea, 7,12-dimethylbenz(a)anthracene, and 3,2'-dimethyl-4-aminobiphenyl after sequential treatment with cyproterone acetate and testosterone propionate. *Cancer Res* **50**, 691-699 (1990).
• Pollard, M., Luckert, P.H. & Schmidt, M.A. Induction of prostate adenocarcinomas in Lobund Wistar rats by testosterone. *Prostate* **3**, 563-568 (1982).
• Wallace, D.C. Mitochondria and cancer. *Nat Rev Cancer* **12**, 685-698 (2012).
• Koc, E.C. et al. Impaired mitochondrial protein synthesis in head and neck squamous cell carcinoma. *Mitochondrion* **24**, 113-121 (2015).
• Kim, H.J., Maiti, P. & Barrientos, A. Mitochondrial ribosomes in cancer. *Semin Cancer Biol* **47**, 6781 (2017).
• Best, C.J. et al. Molecular alterations in primary prostate cancer after androgen ablation therapy. *Clin Cancer Res* **11**, 6823-6834 (2005).
• Kim, J.C. et al. Gene expression profiling: canonical molecular changes and clinicopathological features in sporadic colorectal cancers. *World J Gastroenterol* **14**, 6662-6672 (2008).
• Hardy, S., Wong, N.N., Muller, W.J., Park, M. & Tremblay, M.L. Overexpression of the protein tyrosine phosphatase PRL-2 correlates with breast tumor formation and progression. *Cancer Res* **70**, 8959-8967 (2010).
• Zhou, J., Wang, S., Lu, J., Li, J. & Ding, Y. Over-expression of phosphatase of regenerating liver-3 correlates with tumor progression and poor prognosis in nasopharyngeal carcinoma. *Int J Cancer* **124**, 1879-1886 (2009).
• Xing, X. et al. Phosphatase of regenerating liver-3 (PRL-3) is associated with metastasis and poor prognosis in gastric carcinoma. *J Transl Med* **11**, 309 (2013).
• Vandsemb, E.N. et al. Phosphatase of regenerating liver 3 (PRL-3) is overexpressed in human prostate cancer tissue and promotes growth and migration. *J Transl Med* **14**, 71 (2016).
• Wang, Y. et al. Expression of the human phosphatases of regenerating liver (PRLs) in colonic adenocarcinoma and its correlation with lymph node metastasis. *Int J Colorectal Dis* **22**, 11791184 (2007).
• Stephens, B., Han, H., Hostetter, G., Demeure, M.J. & Von Hoff, D.D. Small interfering RNAmediated knockdown of PRL phosphatases results in altered Akt phosphorylation and reduced clonogenicity of pancreatic cancer cells. *Mol Cancer Ther* **7**, 202-210 (2008).

- Zhao, D. et al. The prognostic significance of protein tyrosine phosphatase 4A2 in breast cancer. *Onco Targets Ther* **8**, 1707-1717 (2015).
- Gao, Y. et al. Over-expression of protein tyrosine phosphatase 4A2 correlates with tumor progression and poor prognosis in nasopharyngeal carcinoma. *Oncotarget* **8**, 77527-77539 (2017).
- Di Stefano, P. et al. The adaptor proteins p140CAP and p130CAS as molecular hubs in cell migration and invasion of cancer cells. *Am J Cancer Res* **1**, 663-673 (2011).
- Damiano, L. et al. p140Cap suppresses the invasive properties of highly metastatic MTLn3-EGFR cells via impaired cortactin phosphorylation. *Oncogene* **31**, 624-633 (2012).
- Kennedy, S. et al. SNIP/p140Cap mRNA expression is an unfavourable prognostic factor in breast cancer and is not expressed in normal breast tissue. *Br J Cancer* **98**, 1641-1645 (2008).
- Di Stefano, P. et al. p140Cap protein suppresses tumour cell properties, regulating Csk and Src kinase activity. *EMBO J* **26**, 2843-2855 (2007).
- Chen, R. et al. Downregulation of SRC Kinase Signaling Inhibitor 1 (SRCIN1) Expression By MicroRNA-32 Promotes Proliferation and Epithelial-Mesenchymal Transition in Human Liver Cancer Cells. *Oncol Res* (2017).
- Zhang, L. et al. Serum MicroRNA-150 Predicts Prognosis for Early-Stage Non-Small Cell Lung Cancer and Promotes Tumor Cell Proliferation by Targeting Tumor Suppressor Gene SRCIN1. *Clin Pharmacol Ther* (2017).
- Wang, P. et al. SRCIN1 Suppressed Osteosarcoma Cell Proliferation and Invasion. *PLoS One* **11**, e0155518 (2016).
- Iovine, B., Iannella, M.L. & Bevilacqua, M.A. Damage-specific DNA binding protein 1 (DDB1) is involved in ubiquitin-mediated proteolysis of p27Kip1 in response to UV irradiation. *Biochimie* **93**, 867-875 (2011).
- Birner, P. et al. Human homologue for Caenorhabditis elegans CUL-4 protein overexpression is associated with malignant potential of epithelial ovarian tumours and poor outcome in carcinoma. *J Clin Pathol* **65**, 507-511 (2012).
- Angers, S. et al. Molecular architecture and assembly of the DDB1-CUL4A ubiquitin ligase machinery. *Nature* **443**, 590-593 (2006).
- Yan, Y., Li, C., Sun, B. & Yang, R. DCAF1 is involved in HCV replication through regulation of miR122. *Arch Virol* **163**, 977-985 (2018).
- Cao, J. et al. The overexpression and prognostic role of DCAF13 in hepatocellular carcinoma. *Tumour Biol* **39**, 1010428317705753 (2017).
- Yan, H. et al. Integrative analysis of multi-omics data reveals distinct impacts of DDB1-CUL4 associated factors in human lung adenocarcinomas. *Sci Rep* **7**, 333 (2017).
- Nakano, K. et al. Identification of androgen-responsive microRNAs and androgen-related genes in breast cancer. *Anticancer Res* **33**, 4811-4819 (2013).
- Han, C.P. et al. Nuclear Receptor Interaction Protein (NRIP) expression assay using human tissue microarray and immunohistochemistry technology confirming nuclear localization. *J Exp Clin Cancer Res* **27**, 25 (2008).
- Chen, H.H. et al. NRIP/DCAF6 stabilizes the androgen receptor protein by displacing DDB2 from the CUL4A-DDB1 E3 ligase complex in prostate cancer. *Oncotarget* **8**, 21501-21515 (2017).
- Bradford, M.M. A rapid and sensitive method for the quantitation of microgram quantities of protein utilizing the principle of protein-dye binding. *Anal Biochem* **72**, 248-254 (1976).
- Laemmli, U.K. Cleavage of structural proteins during the assembly of the head of bacteriophage T4. *Nature* **227**, 680-685 (1970).
- Shevchenko, A. et al. Linking genome and proteome by mass spectrometry: large-scale identification of yeast proteins from two dimensional gels. *Proc Natl Acad Sci U S A* **93**, 1444014445 (1996).

LIST OF FIGURES AND TABLES

Figure 1. Average body weight of rats treated with CA+TP+MNU and control. The number of animals during each sacrifice stage was six. The treated rats showed significant decrease ($p< 0.05$) in body weight in comparison to control.
Figure 2. The dorsolateral prostate lobe weight of rats treated with CA+TP+MNU and control. The treated rats showed significant increase ($p< 0.05$) in organ weight in comparison to control. **Figure 3.** Histological sections of the rat dorsolateral prostate (DLP) after carcinogenesis induction. The photomicrographs A-F represent H&E stained sections of DLP at different time intervals post CA+TP+MNU treatment. (A & B) Normal (Control) dorsolateral prostate post 13 months, showing prostatic acini (x100) of variable sizes within loosely organized fibrous stroma. Epithelium shows normal architecture with intact basement membrane (x400); no inflammatory cell infiltration seen; (C) Treated post 13 months shows benign prostatic hyperplasia (BPH); (D)same section at x400 shows hyperplastic glands with mild variation in nuclear size, no multilayering seen; (E) & (F) shows sections of glands with features of low grade PIN post 15 months, epithelium is projected into the lumen in folds (x100), with some showing multilayering (arrow); enlarged nuclei showing variation in size and shape (anisonucleosis) , absence of nucleoli (x400). PG-Prostate gland, S- Stroma
Figure 4. Histological sections of the rat DLP after carcinogenesis induction. The photomicrographs A-F represent H&E stained sections of DLP at different time intervals post CA+TP+MNU treatment. (C)&(D) showing features of high grade PIN post 17 months of treatment; sections show same features as low grade PIN when viewed in low magnification, however x400 shows hyperchromatic, enlarged nuclei having variation in size and shape, with prominent nucleoli(arrow)- a hallmark of high grade PIN. (A & B) Normal DLP post 19 months lacked any such changes except for some old ages changes, like irregularly infolded epithelial projections in the lumen .Treated post 19 months (E x100, F x400) showing adenocarcinoma of DLP; atypical hyperplastic epithelium, which fuses to form small sheets of cells in some areas (cellular and nuclear pleomorphism); heavy inflammatory infiltrates in the stromal tissue; (F) high power photomicrograph of the lesion from (E) .This lesions demonstrates large dark and irregular shaped nuclei with prominent nucleolus; arrows shows mitotic figures.
Figure 5. One dimensional SDS-PAGE analysis of serum proteins of control (C) and treated samples. Lane M – Molecular weight marker, Lane C – Control (Untreated), Lane T1 & T2 – Treated. Arrows and stars indicate differential protein bands in comparison to control.
Figure 6. Two dimensional gel profile of depleted serum proteome of control (A) and CA+TP+MNU-treated (B) samples obtained by using IEF on pH 4–7 IPG strip and 2-D gel electrophoresis on 12% SDS-PAGE.
Figure 7. (A) PDQuest software generated master gel image containing all the spots respectively obtained in the 2-D gels of control and treated serum sample. (B) 3 D image of the selected spots.
Figure 8. Fresh prostate tissues from rat were processed from untreated (UT) group of animals and treated (post thirteen months;13M-T, fifteen months' treatment; 15-M-T, seventeen months' treatment; 17-M-T, and nineteen months' treatment; 19-M-T) group of animals were used for RNA isolation and cDNA. (A) Differential expression of MRPL15 during time dependent progression of benign infection. (B) Relative expression of MRPL15 in time dependent progression of benign infection. Fold induction was calculated using the $\Delta\Delta C_T$ method of qRTPCR, in which untreated samples were compared to treated samples

relative to HPRT1 levels. Data are presented as means and error bars represent ± SD from five biological replicates/bar. Results are representative of three independent experiments. *P<0.05; **P<0.005 compared with untreated group of animal using paired comparison test of significance through GraphPad Prism version 5.0.

Figure 9. Fresh prostate tissues from rat were processed from untreated (UT) group of animals and treated (post thirteen months;13M-T, fifteen months' treatment; 15-M-T, seventeen months' treatment; 17-M-T, and nineteen months' treatment; 19-M-T) group of animals were used for RNA isolation and cDNA. (A) Differential expression of PTP4A2 during time dependent progression of benign infection. (B) Relative expression of PTP4A2 in time dependent progression of benign infection. Fold induction was calculated using the $\Delta\Delta C_T$ method of qRTPCR, in which untreated samples were compared to treated samples relative to HPRT1 levels. Data are presented as means and error bars represent ± SD from five biological replicates/bar. Results are representative of three independent experiments. *P<0.05; **P<0.005; ***P<0.0005 compared with untreated group of animal using paired comparison test of significance through GraphPad Prism version 5.0.

Figure 10. Fresh prostate tissues from rat were processed from untreated (UT) group of animals and treated (post thirteen months;13M-T, fifteen months' treatment; 15-M-T, seventeen months' treatment; 17-M-T, and nineteen months' treatment; 19-M-T) group of animals were used for RNA isolation and cDNA. (A) Differential expression of SRCIN1 during time dependent progression of benign infection. (B) Relative expression of SRCIN1 in time dependent progression of benign infection. Fold induction was calculated using the $\Delta\Delta C_T$ method of qRTPCR, in which untreated samples were compared to treated samples relative to HPRT1 levels. Data are presented as means and error bars represent ± SD from five biological replicates/bar. Results are representative of three independent experiments. *P<0.05; **P<0.005; ***P<0.0005 compared with untreated group of animal using paired comparison test of significance through GraphPad Prism version 5.0.

Figure 11. Fresh prostate tissues from rat were processed from untreated (UT) group of animals and treated (post thirteen months;13M-T, fifteen months' treatment; 15-M-T, seventeen months' treatment; 17-M-T, and nineteen months' treatment; 19-M-T) group of animals were used for RNA isolation and cDNA. (A) Differential expression of DCAF6 during time dependent progression of benign infection. (B) Relative expression of DCAF6 in time dependent progression of benign infection. Fold induction was calculated using the $\Delta\Delta C_T$ method of qRTPCR, in which untreated samples were compared to treated samples relative to HPRT1 levels. Data are presented as means and error bars represent ± SD from five biological replicates/bar. Results are representative of three independent experiments. *P<0.05; **P<0.005; ***P<0.0005 compared with untreated group of animal using paired comparison test of significance through GraphPad Prism version 5.0.

Table1 SI. List of the primers used in the study.

Table 2 SI Dataset. The MALDI-TOF MS PMF analysis of the protein spots.

Table 3 SI Dataset. Serum proteins. A list of all the peptide sequences, including any deviations from expected cleavage specificity.

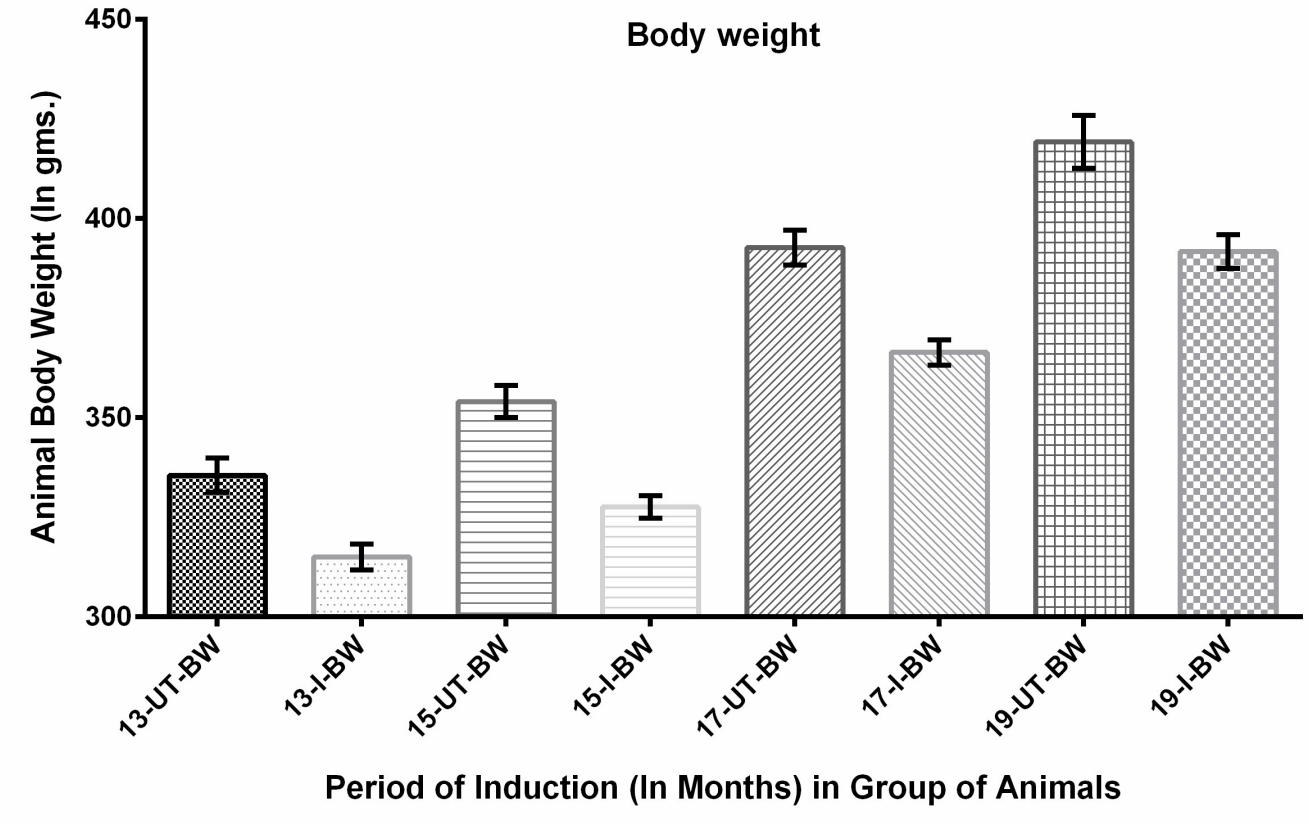

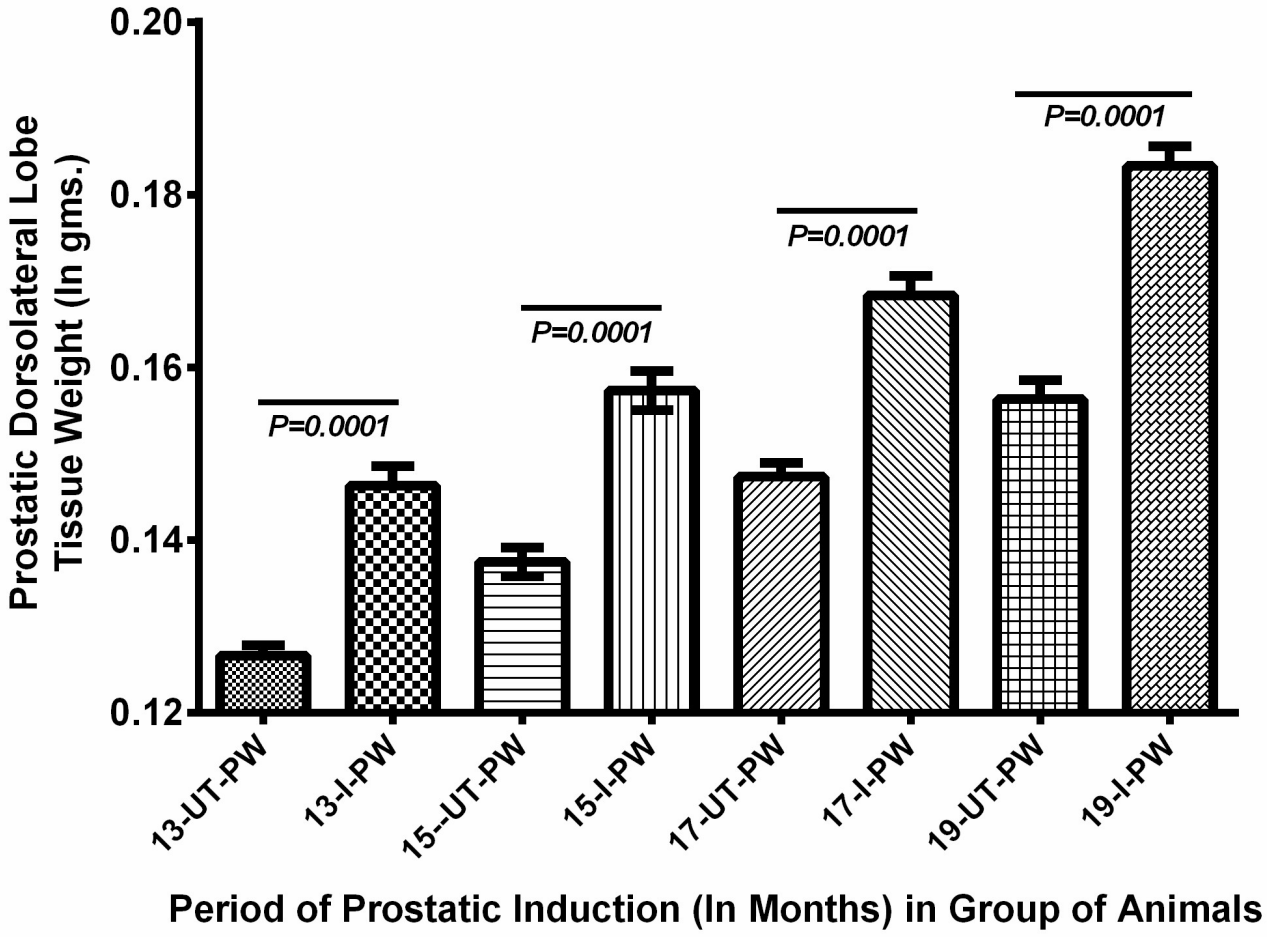
Prostatic Dorsolateral Lobe Tissue Weight (In gms.)
0.20
0.18
0.16
0.14
0.12
P=0.0001
P=0.0001
P=0.0001
P=0.0001
13-UT-PW
13-I-PW
15--UT-PW
15-I-PW
17-UT-PW
17-I-PW
19-UT-PW
19-I-PW
Period of Prostatic Induction (In Months) in Group of Animals

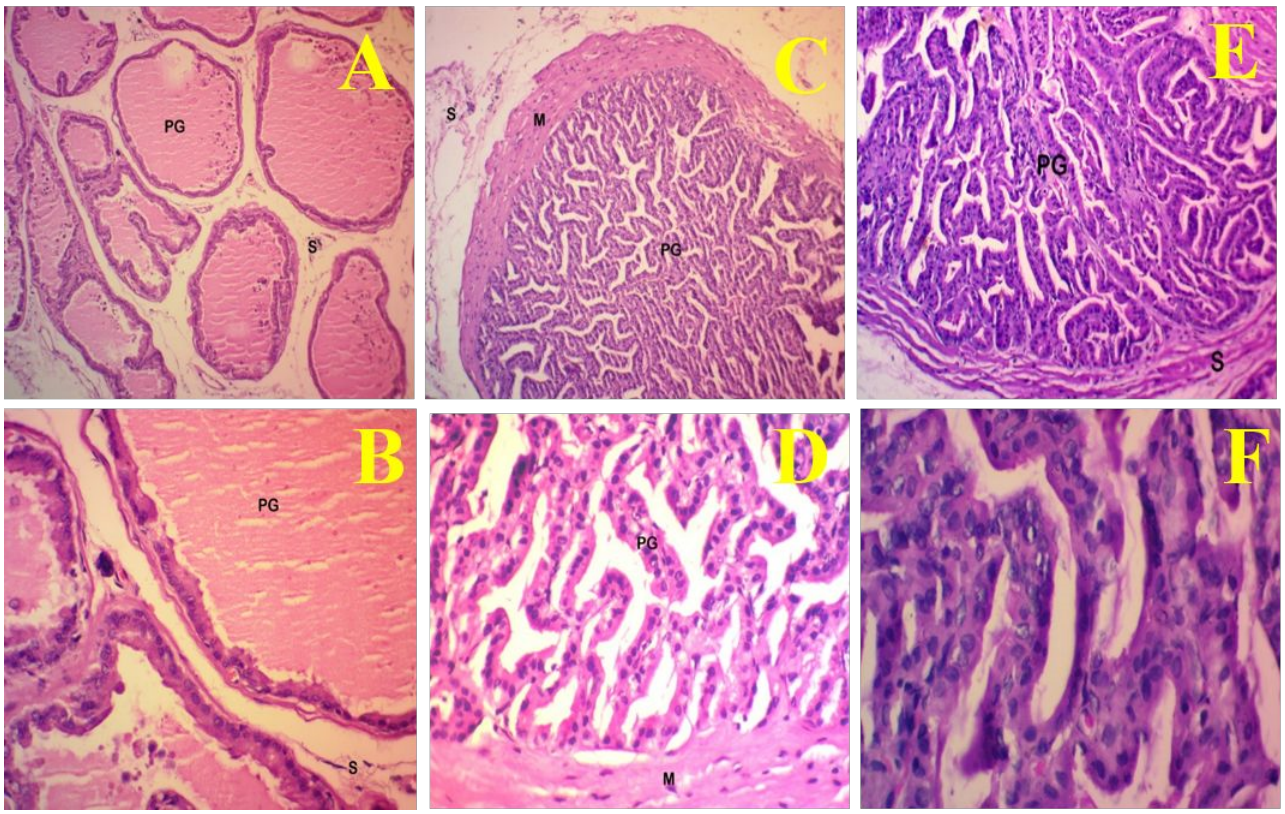
A
PG
S
C
S
M
PG
E
PG
S
B
PG
S
D
PG
M
F

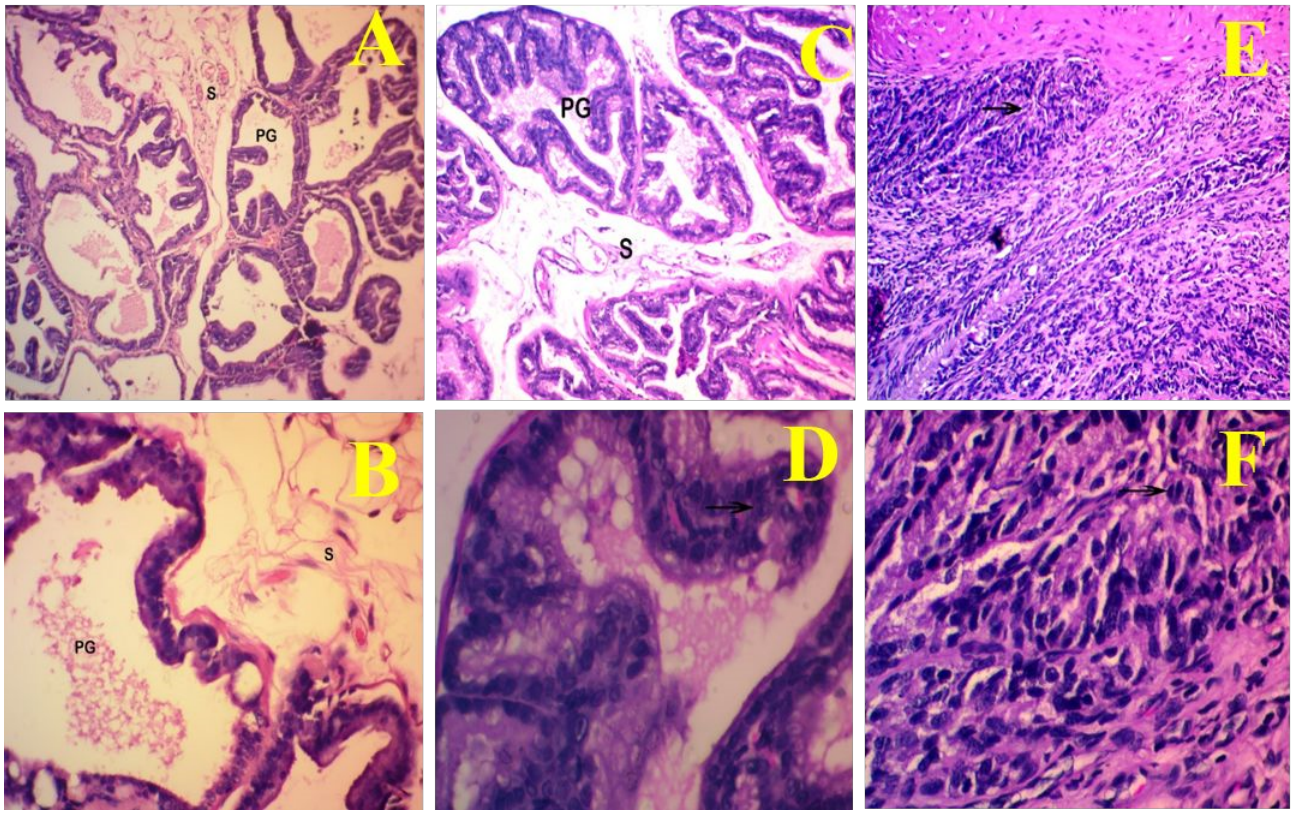
A
S
PG
C
PG
S
E
B
S
PG
D
F

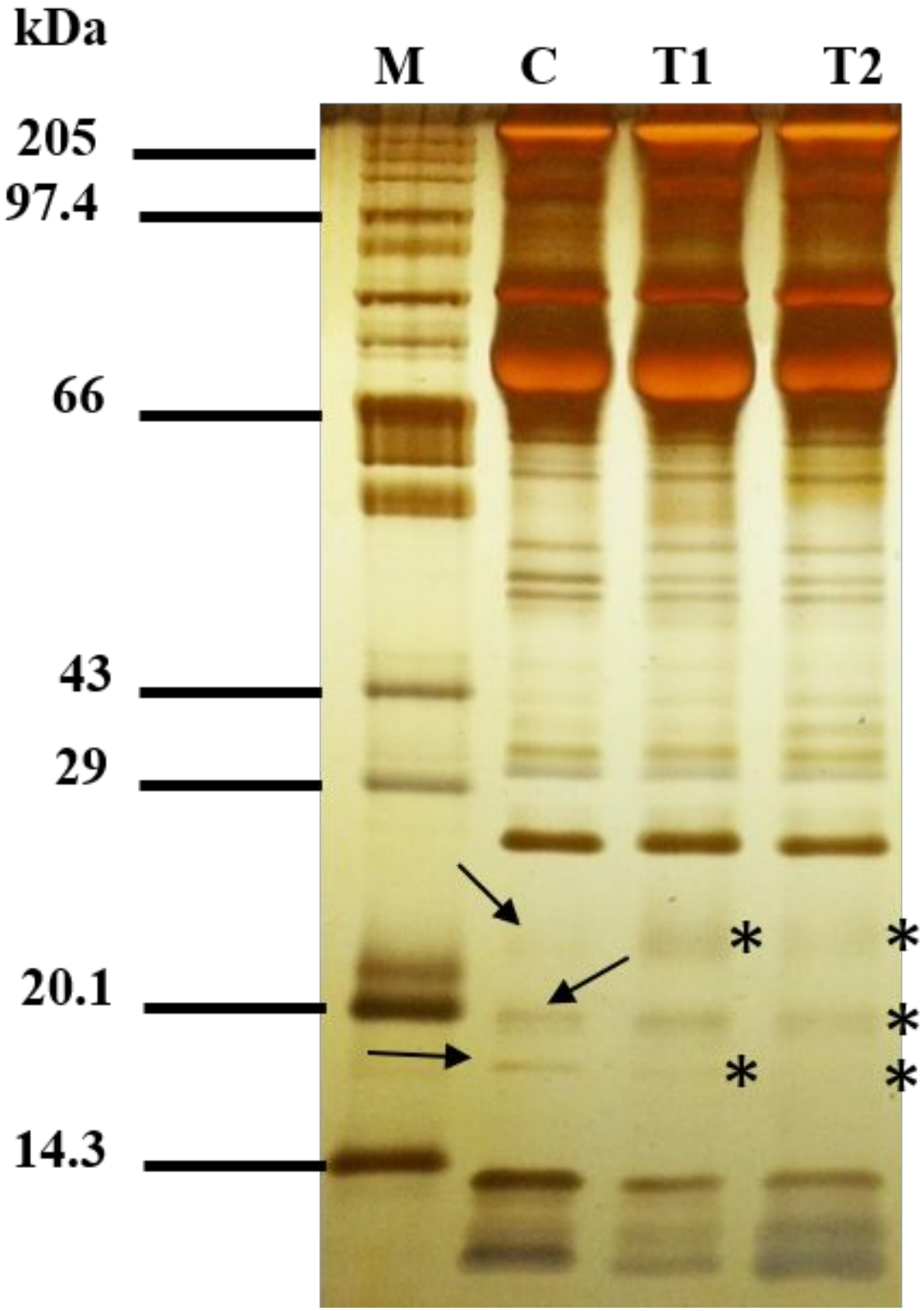
kDa
M
C
T1
T2
205
97.4
66
43
29
20.1
14.3

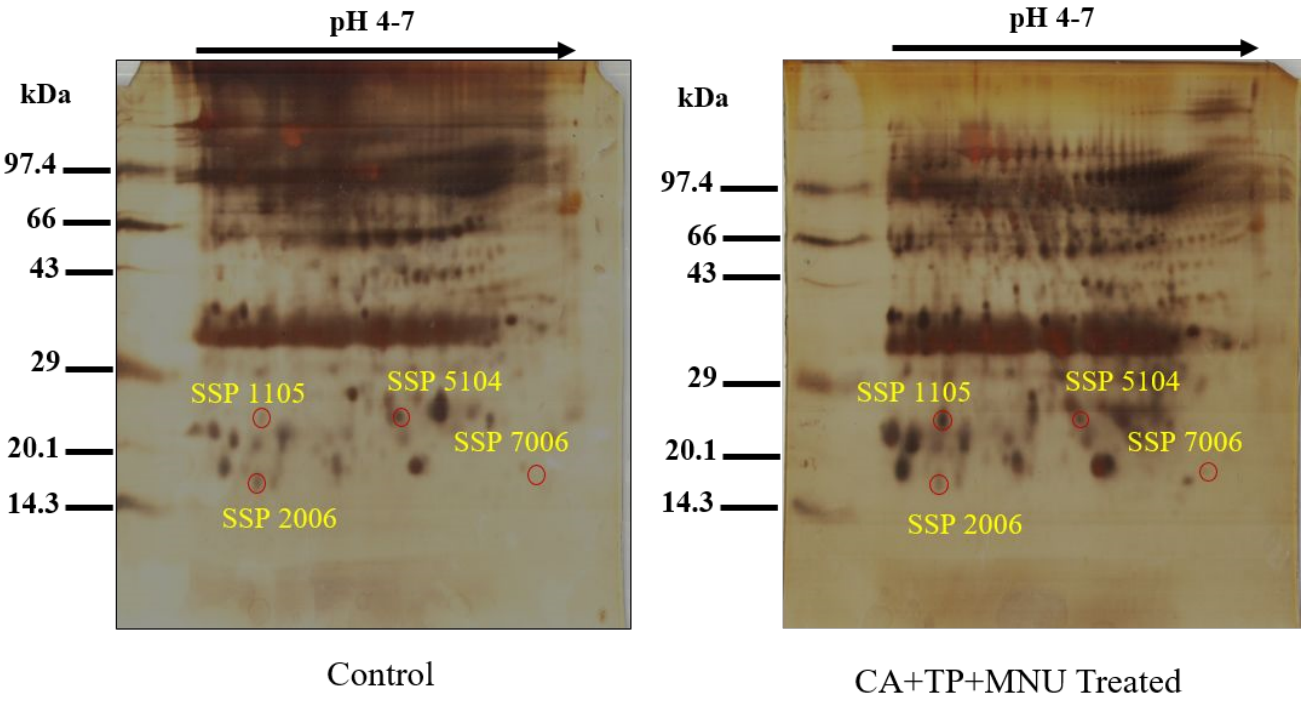
pH 4-7
kDa
97.4
66
43
29
20.1
14.3
SSP 1105
SSP 5104
SSP 7006
SSP 2006
Control
pH 4-7
kDa
97.4
66
43
29
20.1
14.3
SSP 1105
SSP 5104
SSP 7006
SSP 2006
CA+TP+MNU Treated

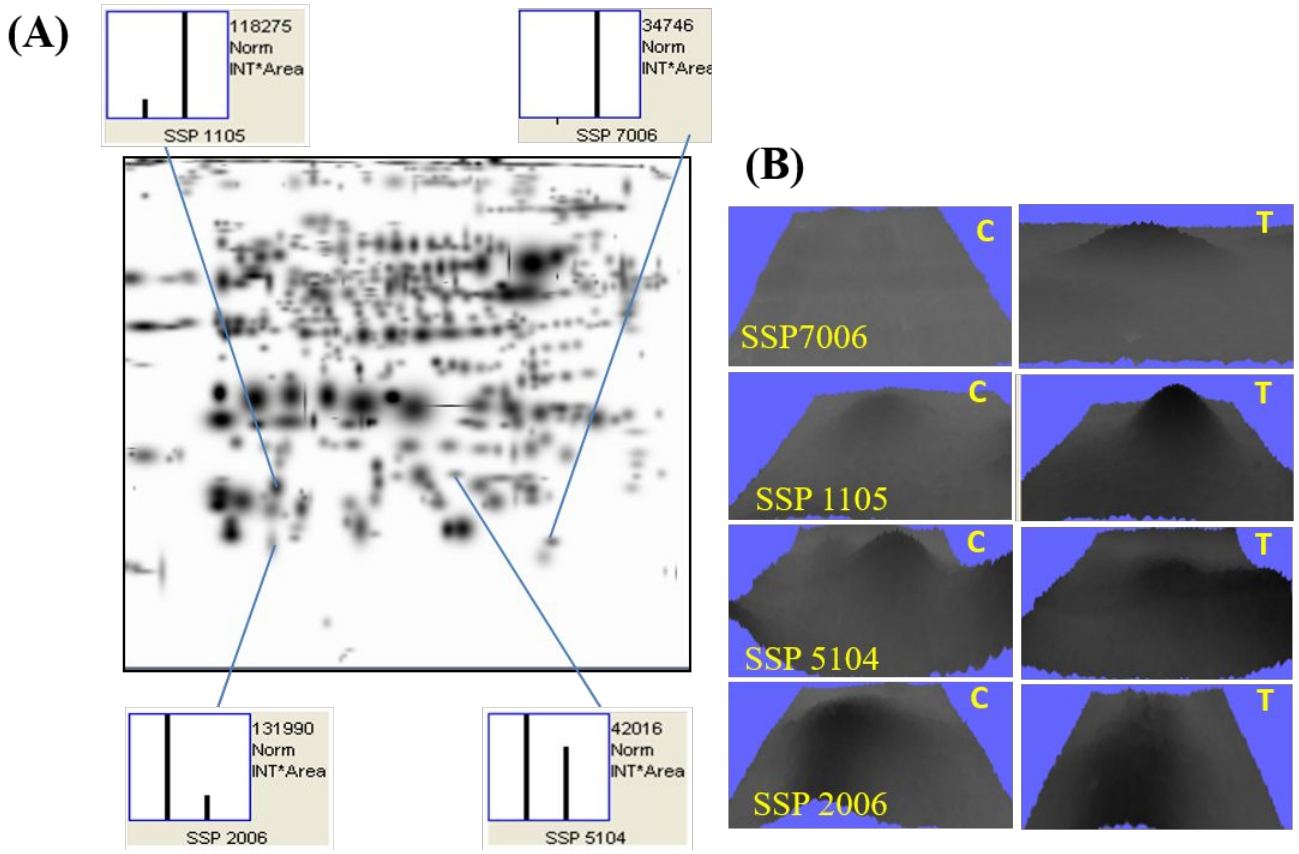
(A)
118275
Norm
INT*Area
SSP 1105
34746
Norm
INT*Area
SSP 7006
131990
Norm
INT*Area
SSP 2006
42016
Norm
INT*Area
SSP 5104
(B)
C
T
SSP7006
SSP 1105
SSP 5104
SSP 2006

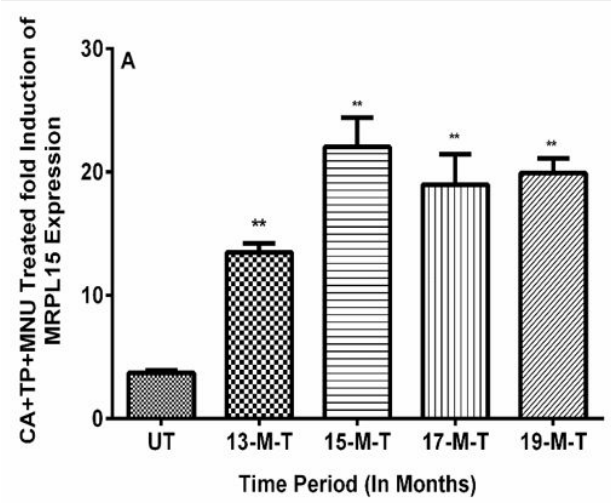
A
CA+TP+MNU Treated fold Induction of MRPL15 Expression
30
20
10
0
**
**
**
**
UT
13-M-T
15-M-T
17-M-T
19-M-T
Time Period (In Months)

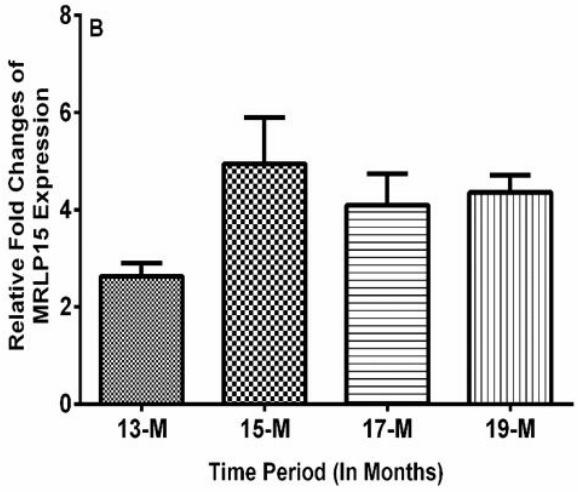
B
Relative Fold Changes of MRLP15 Expression
8
6
4
2
0
13-M
15-M
17-M
19-M
Time Period (In Months)

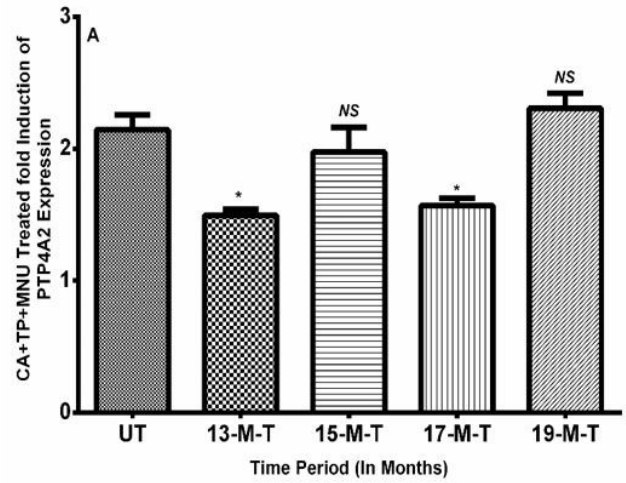
A
CA+TP+MNU Treated fold Induction of PTP4A2 Expression
3
2
1
0
*
NS
*
NS
UT
13-M-T
15-M-T
17-M-T
19-M-T
Time Period (In Months)

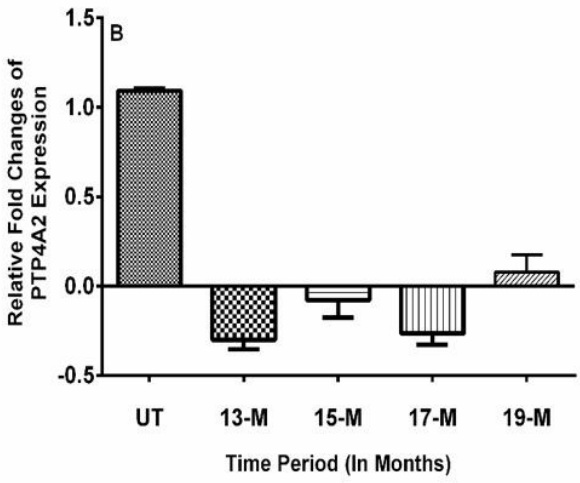
B
Relative Fold Changes of PTP4A2 Expression
1.5
1.0
0.5
0.0
-0.5
UT
13-M
15-M
17-M
19-M
Time Period (In Months)

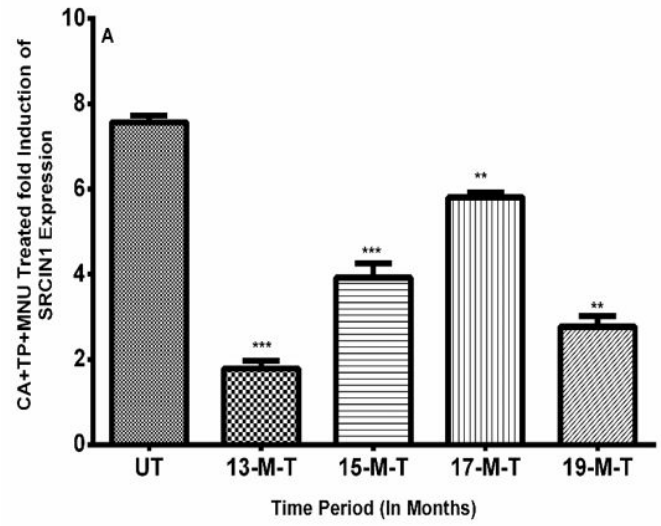
A
CA+TP+MNU Treated fold Induction of SRCIN1 Expression
10
8
6
4
2
0
***
***
**
**
UT
13-M-T
15-M-T
17-M-T
19-M-T
Time Period (In Months)

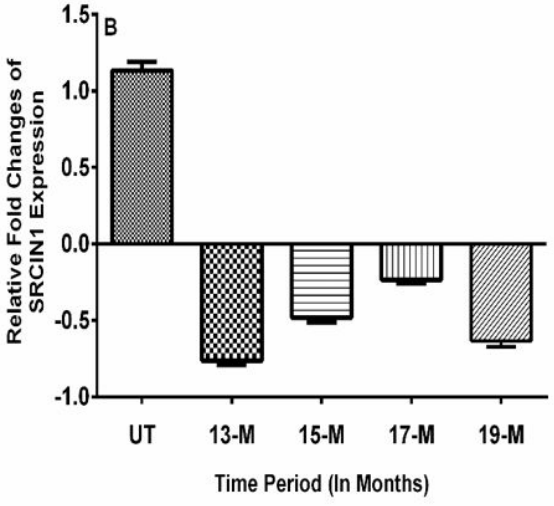
B
Relative Fold Changes of SRCIN1 Expression
1.5
1.0
0.5
0.0
-0.5
-1.0
UT
13-M
15-M
17-M
19-M
Time Period (In Months)

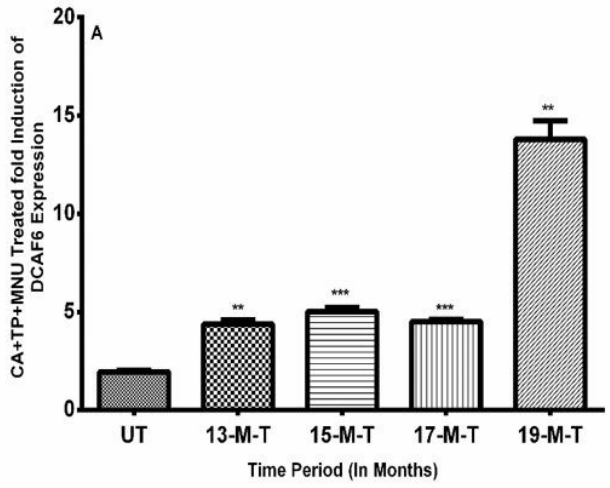
A
CA+TP+MNU Treated fold Induction of DCAF6 Expression
20
15
10
5
0
**
***
***
**
UT
13-M-T
15-M-T
17-M-T
19-M-T
Time Period (In Months)

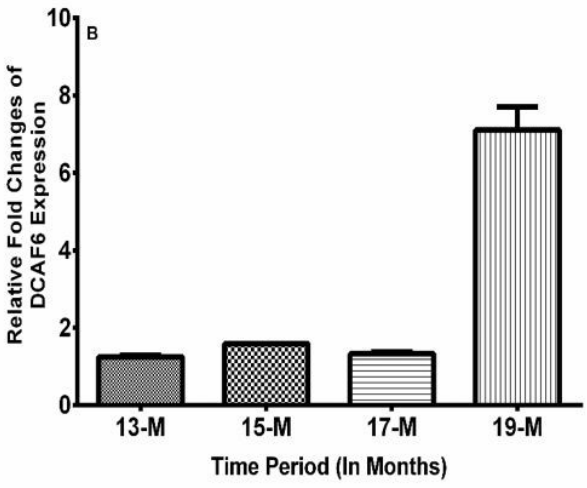
B
Relative Fold Changes of DCAF6 Expression
10
8
6
4
2
0
13-M
15-M
17-M
19-M
Time Period (In Months)